Spiropyran Photoisomerization Dynamics in Multiresponsive Hydrogels

Meeks, Amos; Lerch, Michael M.; Schroeder, Thomas B.H.; Shastri, Ankita; Aizenberg, Joanna

Published in:
Journal of the American Chemical Society

DOI:
10.1021/jacs.1c08778

Publication date:
2022

JACS
JOURNAL OF THE AMERICAN CHEMICAL SOCIETY
pubs.acs.org/JACS
Article

Spiropyran Photoisomerization Dynamics in Multiresponsive Hydrogels

Amos Meeks, Michael M. Lerch, Thomas B. H. Schroeder, Ankita Shastri, and Joanna Aizenberg*

Cite This: J. Am. Chem. Soc. 2022, 144, 219−227
Read Online

ABSTRACT: Light-responsive, spiropyran-functionalized hydrogels have been used to create reversibly photoactuated structures for applications ranging from microfluidics to nonlinear optics. Tailoring a spiropyran-functionalized hydrogel system for a particular application requires an understanding of how co-monomer composition affects the switching dynamics of the spiropyran chromophore. Such gels are frequently designed to be responsive to different stimuli such as light, temperature, and pH. The coupling of these influences can significantly alter spiropyran behavior in ways not currently well understood. To better understand the influence of responsive co-monomers on the spiropyran isomerization dynamics, we use UV−vis spectroscopy and time-dependent fluorescence intensity measurements to study spiropyran-modified hydrogels polymerized from four common hydrogel precursors of different pH and temperature responsivity: acrylamide, acrylic acid, *N*-isopropylacrylamide, and 2-(dimethylamino)-ethyl methacrylate. In acidic and neutral gels, we observe unusual nonmonotonic, triexponential fluorescence dynamics under 405 nm irradiation that cannot be explicated by either the established spiropyran−merocyanine interconversion model or hydrolysis. To explain these results, we introduce an analytical model of spiropyran interconversions that includes H-aggregated merocyanine and its light-triggered disaggregation under 405 nm irradiation. This model provides an excellent fit to the observed fluorescence dynamics and elucidates exactly how creating an acidic internal gel environment promotes the fast and complete conversion of the hydrophilic merocyanine speciesto the hydrophobic spiropyran form, which is desired in most light-sensitive hydrogel actuators. This can be achieved by incorporating acrylic acid monomers and by minimizing the aggregate concentration. Beyond spiropyran-functionalized gel actuators, these conclusions are particularly critical for nonlinear optical computing applications.

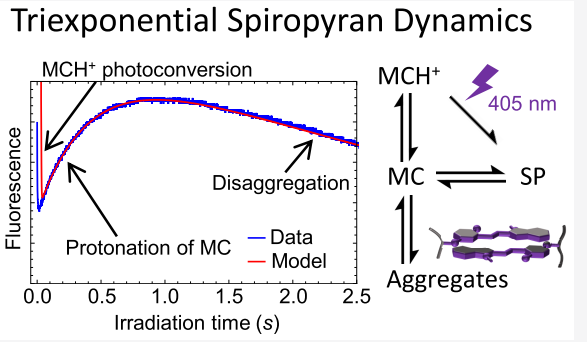

INTRODUCTION

Photoresponsive hydrogels have found applications in a wide variety of fields, including microfluidics,[1−5] soft robotic walkers,[6] tools for mechanical interactions with biological matter,[7] switchable surfaces,[8−11] data storage,[12] drug delivery,[13] and as a nonlinear optical material.[14,15] The spiropyran photoswitch is commonly used to impart light sensitivity to hydrogels due to the reversible changes in molecular structure, charge, and hydrophobicity it undergoes in response to visible light irradiation.[16] Commonly, spiropyran pendant moieties are directly tethered to the polymer backbone.[16−18] Under acidic aqueous conditions these moieties exist primarily in the charged, protonated, ring-open merocyanine (MCH^+) form. Irradiation with visible light triggers deprotonation and ring closure to the uncharged, relatively hydrophobic spiropyran (SP) form, which causes the gel to expel water and contract due to the increased hydrophobicity of the polymer backbone. The thermally unstable SP isomer spontaneously reopens to the zwitterionic merocyanine (MC) form in aqueous environments,[19] which is then reprotonated to form MCH^+, returning the hydrogel to its swollen state. The ring-opening of SP can also be accelerated by irradiation with UV light.[16,20] Recent work has underscored the importance of charge in determining the response of the hydrogel to spiropyran isomerization, as introducing negatively charged sulfonic acid groups to the spiropyran moiety can flip the hydrogel's response such that it swells upon irradiation with visible light rather than contracting.[18] Different types of spiropyran-functionalized hydrogels can be designed to undergo volume changes of around 100% upon irradiation[17,18] and have successfully been used for light-responsive microfluidic valves[1,2] and soft robotic walkers.[6]

In order to achieve large responses to visible light irradiation, spiropyran monomers are frequently combined with co-monomers that impart responsivity to other stimuli such as temperature and pH, enabling cooperative effects.[21−24] For

Received: August 19, 2021
Published: December 29, 2021

https://doi.org/10.1021/jacs.1c08778
J. Am. Chem. Soc. 2022, 144, 219−227

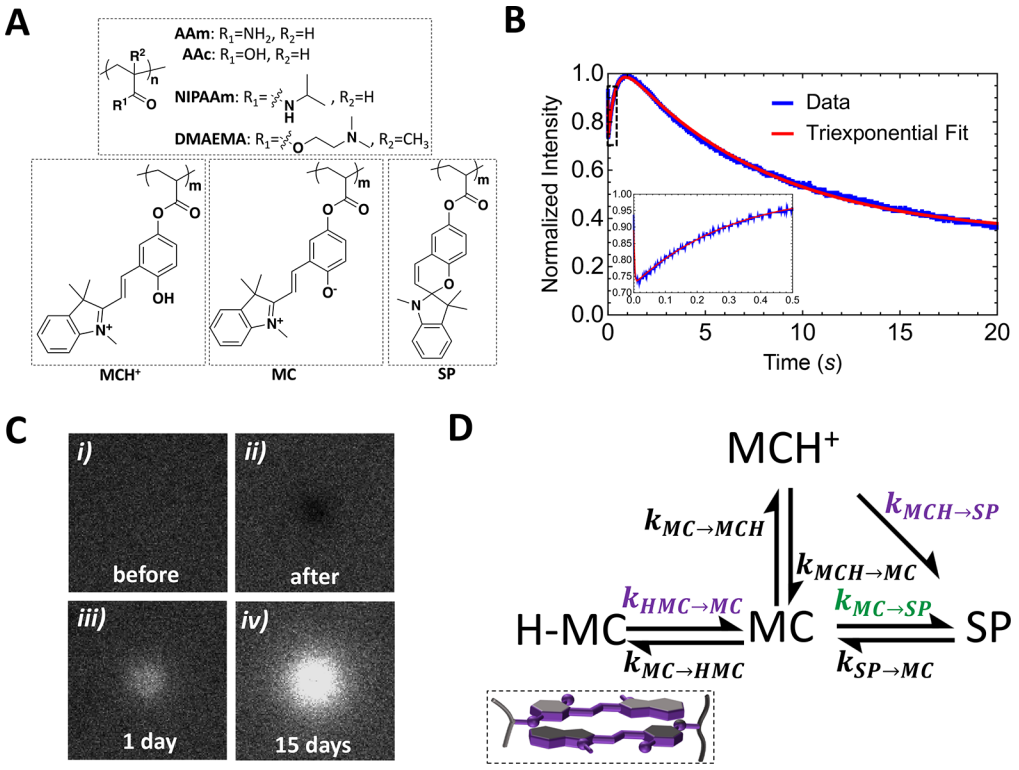

Figure 1. Probing spiropyran switching dynamics with confocal fluorescence microscopy. (A) Chemical composition of studied hydrogel networks: polyacrylamide (pAAm), poly(acrylic acid) (pAAc), poly(*N*-isopropylacrylamide) (pNIPAAm), and poly(2-(dimethylaminoethyl)methacrylate) (pDMAEMA) based cross-linked networks with covalently attached spiropyran. The predominant chromophore states include ring-closed spiropyran (SP), ring-open merocyanine (MC), and protonated merocyanine (MCH^+). (B) 525−575 nm fluorescence intensity data (blue line) of a spot under continuous high-intensity 405 nm excitation in a poly(AAc-*co*-SP) hydrogel immersed in deionized water (DIW). Inset shows the first 0.5 s to highlight the initial drop and then increase of intensity. The intensity profile is nonmonotonic and is well fit by a triexponential function (red line). A traditional mass-conserving system comprising only linear interconversion reactions between SP, MC, and MCH^+ cannot lead to triexponential dynamics. (C) 561 nm fluorescence images of before and after 40 s high-intensity 405 nm irradiation of a spot in a poly(AAc-*co*-SP) hydrogel: (i) region immediately before exposure to high-intensity light; (ii) loss of fluorescence in the irradiated spot immediately after exposure; (iii) same spot 1 day later; (iv) same spot 15 days later. A clear increase in fluorescence is discernible. All images are 150 μm by 150 μm. (D) Reaction scheme including H-aggregated MC (H-MC, inset) that we propose to explain the observed triexponential and long-term dynamics. The labels for rate constants used in this work are written next to the corresponding arrow, and violet-colored rate constants ($k_{MCH\rightarrow SP}$ and $k_{HMC\rightarrow MC}$) indicate a dependence on 405 nm light intensity, while the green rate constant ($k_{MC\rightarrow SP}$) indicates a dependence on 561 nm light intensity. Inset shows a schematic representation of H-aggregated MC attached to a polymer backbone.

example, temperature-responsive *N*-isopropylacrylamide (NIPAAm) is commonly employed in hydrogels to instill a swollen-to-collapsed-phase transition upon heating above the lower critical solution temperature (LCST) of the hydrogel. Such a transition can be coupled to spiropyran photoswitching such that the change in hydrophobicity accompanying conversion of spiropyran from MCH^+ to SP lowers the LCST of the NIPAAm-spiropyran copolymers by about 10 °C,[21] which can result in a large volume change upon irradiation for gels near the critical temperature. In other instances, by introducing spiropyran moieties into a pH-responsive acrylic acid (AAc)-based hydrogel, one can create the acidic environment necessary to generate a large concentration of MCH^+ [17] while also making the gel responsive to the change in pH that occurs due to the light-driven transformation of MCH^+ to SP.[25] Given the large number of possible ways to impart a polymer system with sensitivity to different stimuli, there is tremendous potential in coupling spiropyran moieties with a large number of different co-monomers to elicit a desired response for a given environment.

However, the rational design of such multifunctional hydrogels requires an understanding of how the choice of specific co-monomers affects the interconversion dynamics between different states of the spiropyran moieties. While significant work has been done to understand the effects of the spiropyran molecular structure on its photochemistry in solution[1,10,18,26−30] and on the effects of incorporation into a dense polymer matrix,[31] less work has been done to explore the effects that co-monomers in an aqueous hydrogel environment have on spiropyran dynamics.[24,32] Additionally, the high-intensity, focused laser light conditions relevant to the nonlinear optics of spiropyran-functionalized hydrogels[14,15] constitute an environment in which spiropyran switching kinetics have rarely been studied. As part of our ongoing efforts to codify design principles for hydrogels that achieve self-regulation via opto-chemo-mechanical feedback behaviors,[14,15,33−37] we used laser scanning confocal fluorescence microscopy and UV−vis spectroscopy to probe the effects of different co-monomers on the dynamics of light-driven and thermal isomerization of the spiropyran moieties within four different commonly used hydrogel materials: temperature-responsive pNIPAAm gels, pH-responsive pAAc and poly(2-

https://doi.org/10.1021/jacs.1c08778
J. Am. Chem. Soc. 2022, 144, 219−227

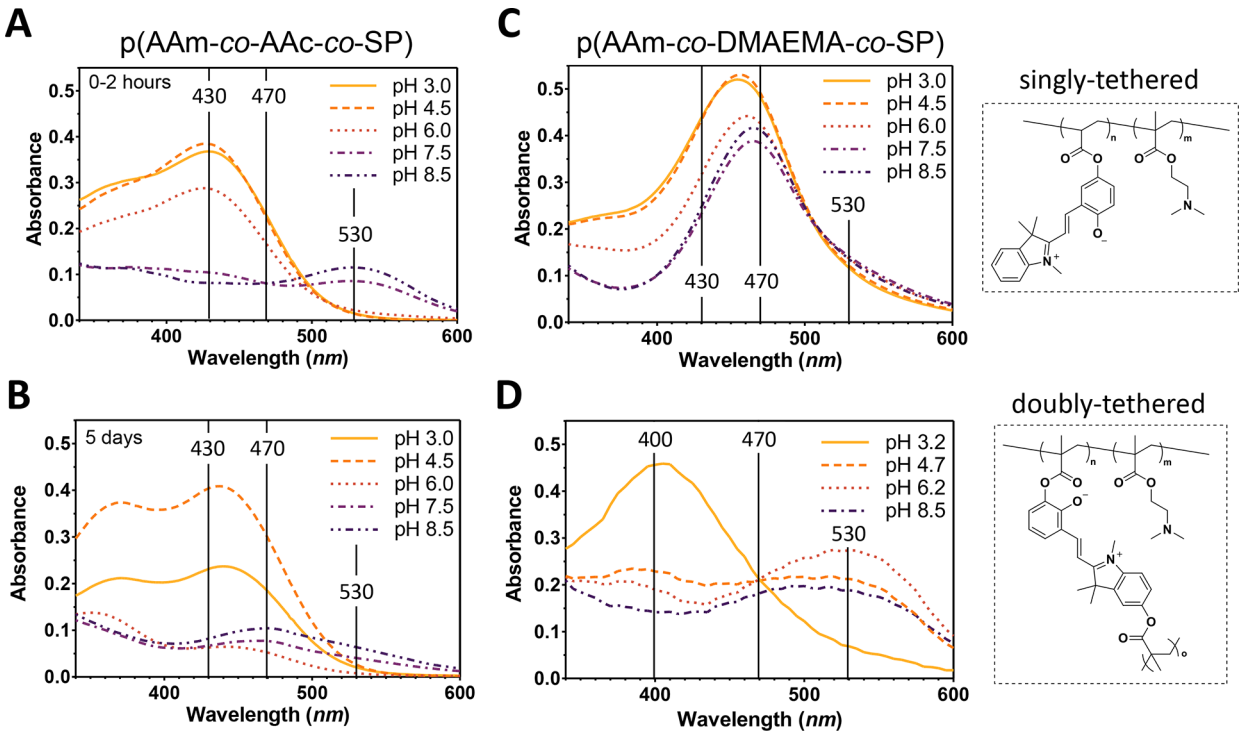

Figure 2. Experimental support for H-aggregated MC in spiropyran-functionalized hydrogels. (A) UV−vis spectra of linear spiropyran-functionalized poly(AAm-*co*-AAc-*co*-SP) polymers freshly (0−2 h) dissolved in buffered solutions (0.2 M citrate or phosphate) with pH ranging from 3.0 to 8.5. We assign the $\lambda_{max} \sim 530$ nm absorption band to MC, while we assign the $\lambda_{max} \sim 430$ nm band to MCH^+.[1,16,17,24] (B) UV−vis spectra of the same solutions shown in (A) taken 5 days later. The 530 nm band observed under neutral to basic conditions is now observed to blue-shift to about 470 nm, which we assign to H-aggregated MC. (C) UV−vis spectra of spiropyran pendant un-cross-linked poly(AAm-*co*-DMAEMA-*co*-SP) polymers dissolved in buffered solutions of pH ranging from 3.0 to 8.5. The two main peaks observed in poly(AAm-*co*-AAc-*co*-SP) polymers are replaced by a single peak at about 460−470 nm, even under acidic conditions. (D) Additional support is found in spiropyran-cross-linked poly(AAm-*co*-DMAEMA) hydrogels.[37] Such hydrogels show absorption bands at $\lambda_{max} \sim 400$ nm and $\lambda_{max} \sim 530$ nm corresponding to the MCH^+ and MC-species, respectively, when immersed in phosphate buffers (0.05 M). No broad absorption at 470 nm is observed.[37] In the context of possible H-MC aggregates, we propose that lack of a $\lambda_{max} \sim 470$ nm absorption band is due to the tethering constraints inhibiting the aggregation of MC.

(dimethylamino)methacrylate) (pDMAEMA) gels, and non-responsive polyacrylamide (pAAm) gels. These gels differ significantly in terms of charge, acidity, and hydrophobicity and thus provide a good platform to study spiropyran behavior in a wide variety of practical hydrogel environments. We observed significant differences in the photoswitch conversion dynamics between different gels that are well-explained by the different internal pH environments. In addition, however, we also noticed unexpected dynamics in all gels that cannot be explained by interconversions within the MCH^+/MC/SP system outlined above. Considering irreversible hydrolytic[26,27,38,39] or photodegradation[38] pathways also cannot explain the dynamics. The nonmonotonic, triexponential fluorescence dynamics we observe can only be rationalized by invoking an additional photoisomerizing species. Previous reports have described the formation of light-responsive MC aggregates in homopolymers[40,41] and hydrogels in some instances,[24] leading us to hypothesize that the incorporation and dispersion of dye molecules from such aggregates may be responsible for the complexity of the photoresponse. On the basis of these observations and a new analytical model that includes (dis)aggregation, we conclude that while controlling the internal gel pH is the most significant factor when designing multiresponsive spiropyran-functionalized hydrogels, aggregation must also be considered when optimizing for the fastest and most significant photoresponse.

RESULTS AND DISCUSSION

Observation of Unexpected Dynamics in Spiropyran Switching. Spiropyran-functionalized hydrogels were prepared by free radical UV copolymerization of an approximately 40 wt% monomer (AAc, NIPAAm, AAm, or DMAEMA) and 0.49 wt% acrylated spiropyran solution (Figure 1A, Supporting Information sections S1−S3). We used laser scanning confocal microscopy to indirectly probe the spiropyran isomerization dynamics in each separate gel material immersed in deionized water (DIW). We measured the spiropyran fluorescence dynamics under high-intensity light (a ∼5 mW laser focused to roughly 20 μm resulting in ∼800 W/cm^2 peak intensity) at microsecond temporal resolution and used excitation wavelengths of 561 and 405 nm in order to separately excite the MC ($\lambda_{max} \approx 530$ nm) and MCH^+ ($\lambda_{max} \approx 430$ nm) forms.[1,16,17,24] In a typical high-intensity experiment, we would constantly irradiate a sample for a duration of up to two minutes with a focused laser and measure the changes in fluorescence signal in the corresponding emission window for MC (λ_{ex} = 561 nm, ∼5.5 mW, λ_{em} = 625−675 nm) or MCH^+ (λ_{ex} = 405 nm, ∼4.7 mW, λ_{em} = 525−575 nm). Recovery kinetics were then measured by excitation with a low-power (μW) laser rastered quickly over a 1.3 mm by 1.3 mm area, repeated with long (seconds to days) periods of darkness between data collection. The fluorescence signal from the region that underwent constant high-intensity irradiation from

https://doi.org/10.1021/jacs.1c08778
J. Am. Chem. Soc. 2022, 144, 219−227

the focused beam was compared to the background to provide a control for the fluorescence dynamics in the absence of high-intensity irradiation. See Supporting Information section S1.3 and Scheme S1 for more experimental details.

Under high-intensity irradiation of MC with 561 nm light, we observe biexponential photoisomerization kinetics, which we ascribe to the combined rates of MC to SP photoisomerization and MCH^+ deprotonation, and single exponential recovery in the dark, which we ascribe to the spontaneous ring-opening of SP (Supporting Information section S4). In contrast, high-intensity 405 nm irradiation in spiropyran-containing pAAc, pNIPAAm, and pAAm gels leads to unexpected triexponential, nonmonotonic photoconversion kinetics, where fluorescence first rapidly decreases and then increases at a slower rate before decreasing again (Figure 1B). Following the traditional SP, MC, and MCH^+ model of interconversions, one would again expect biexponential dynamics arising from the rates of MCH^+ photoconversion and MC protonation, contrary to what was observed.

We further note an unexpected, slow increase in fluorescence signal in the 625−675 nm window (λ_{ex} = 561 nm) in the previously irradiated regions of these samples that persists for up to a month after high-intensity 405 nm irradiation, resulting ultimately in a strongly fluorescent spot compared to the gel background (Figure 1C, Supporting Information section S5). This long-time scale recovery dynamics is not commensurate with the several minute time scale for the recovery of fluorescence after high-intensity 561 nm irradiation (Supporting Information section S4.2). Taken together with the triexponential dynamics observed under 405 nm irradiation, these results strongly suggest that an additional spiropyran-based species exists in the spiropyran-functionalized gel system and that it undergoes reactions predominantly at longer time scales or under intense 405 nm irradiation. This is a significant departure from prior work on spiropyran-functionalized hydrogels, which only considers interconversion reactions involving MCH^+, MC, and SP[1,5,6,8,10,14,16−18,42,43] or spiropyran hydrolysis.[26,27,38,39]

We hypothesize that this fourth species consists of H-aggregated merocyanine stacks (H-MC) between covalently attached spiropyrans, which disaggregate upon exposure to intense 405 nm light[41,44] and which slowly re-form at long time scales (Figure 1D). Even at low concentrations, merocyanine dyes of all types are consistently observed to form H-aggregates, where the zwitterionic dyes align their dipoles by stacking with opposite alignment, and J-aggregates, where positively and negatively charged ends are joined such that all molecules have the same alignment.[16,45] In particular, H-aggregates have been identified in spiropyran pendant group homopolymers dissolved in toluene based on the observation of an absorption peak blue-shifted by roughly 20 nm from the main MC peak that shows slower kinetics under visible light irradiation than the MC peak.[41,46] These homopolymers have been directly observed to crystallize into a zipper-like structure in which long stacks of H-aggregated merocyanines bind together two separate polymer backbones.[40] In bilayer membranes, larger spectral shifts of up to roughly 70 nm have been observed,[47] and light-responsive merocyanine H-aggregates have also been identified by secondary peaks blue-shifted by about 35 nm from the MC peak in poly(DMAEMA-*co*-SP) polymers in a variety of solvents.[24]

Experimental Support for the Formation of Aggregates. We find support for the existence of H-MC in the UV−vis spectra of un-cross-linked spiropyran-functionalized polymers upon aging. Figure 2A shows UV−vis spectra for linear poly(AAm-*co*-AAc-*co*-SP) dissolved in solutions buffered (0.2 M citrate or phosphate buffer) between pH 3.0 and pH 8.5. These spectra were taken between zero and 2 h after adding the respective aqueous polymer solutions into a pH-buffered solution. Under neutral to basic conditions, we observe a peak at 530 nm (and minor peak at ∼370 nm), which is generally ascribed to the MC isomer (and its chromene part). At lower pH the absorption peak at 430 nm corresponds to the MCH^+ form. There is also a weak 370 nm absorption band that increases in intensity upon sample aging, which could correspond to partial hydrolysis of the spiropyran moiety, a *cis*-MCH^+ species,[28] or the quinoidal form of the MC species.[24] These identifications align well with the previous literature.[1,16,17,24]

Figure 2B shows UV−vis spectra of the same solutions 5 days later. We observe that in the solutions at pH 6 or higher the peak at 530 nm shifts toward a broad band centered about 470 nm. We hypothesize that the peak at 470 nm represents a blue shift of the 530 nm MC peak due to the formation of H-aggregates.[24,41,45,46] UV−vis spectra of spiropyran-functionalized poly(AAm-*co*-DMAEMA-*co*-SP) un-cross-linked polymers (Figure 2C) further corroborate this hypothesis: the internal pH of DMAEMA-based gels is strongly basic even at relatively low external solution pH (Supporting Information section S7.3), and correspondingly the spectra show a broad absorption band around 470 nm at a similar position to the proposed H-MC peak in the aged linear polymer samples. SAXS and WAXS experiments on two-year-old spiropyran-functionalized poly(AAm-*co*-DMAEMA) gels show sharp peaks suggestive of crystallinity (Supporting Information section S6), providing further support for the slow formation of aggregates. In addition, our own work on bis-acrylated spiropyran cross-linkers[37] provides more circumstantial support for the H-MC hypothesis: a bis-acrylated spiropyran acting as a cross-linker would not be expected to form aggregates due to the steric constraints on both ends of the chromophore. Indeed, in UV−vis spectra of spiropyran-cross-linked poly(AAm-*co*-DMAEMA-*co*-SP) hydrogels there is no evidence of a peak at 470 nm (Figure 2D). Instead, the peaks correspond to MC (λ_{max} ∼ 530 nm) and MCH^+ (λ_{max} ∼ 400 nm).

Theoretical Model of Photoswitching Dynamics in Spiropyran-Functionalized Hydrogels. We hypothesized that expanding the three-species SP/MC/MCH^+ system to include an additional spiropyran species (H-MC) might allow us to reconcile our observations of both the triexponential fluorescence kinetics and the absorbance peak at 470 nm. We therefore developed an analytical model (Figure 1D) to test whether the aggregation hypothesis could plausibly account for the observed spiropyran isomerization dynamics across a range of responsive hydrogel materials. In our model MC and MCH^+ interconvert as a function of the solution pH with a pK_a of ∼7, set to be independent of the co-monomer (Supporting Information Figure S8).[28] MC and SP form an equilibrium that is shifted toward SP depending on the intensity of 561 nm light, while MCH^+ is converted to SP at a rate that depends on the intensity of 405 nm light. We also include H-MC at an initial concentration that, due to the very slow aggregation dynamics in the dark, is not necessarily equilibrated with MC and which has a rate of disaggregation that increases under irradiation with 405 nm light. We assume that the breadth of

https://doi.org/10.1021/jacs.1c08778
J. Am. Chem. Soc. 2022, 144, 219−227

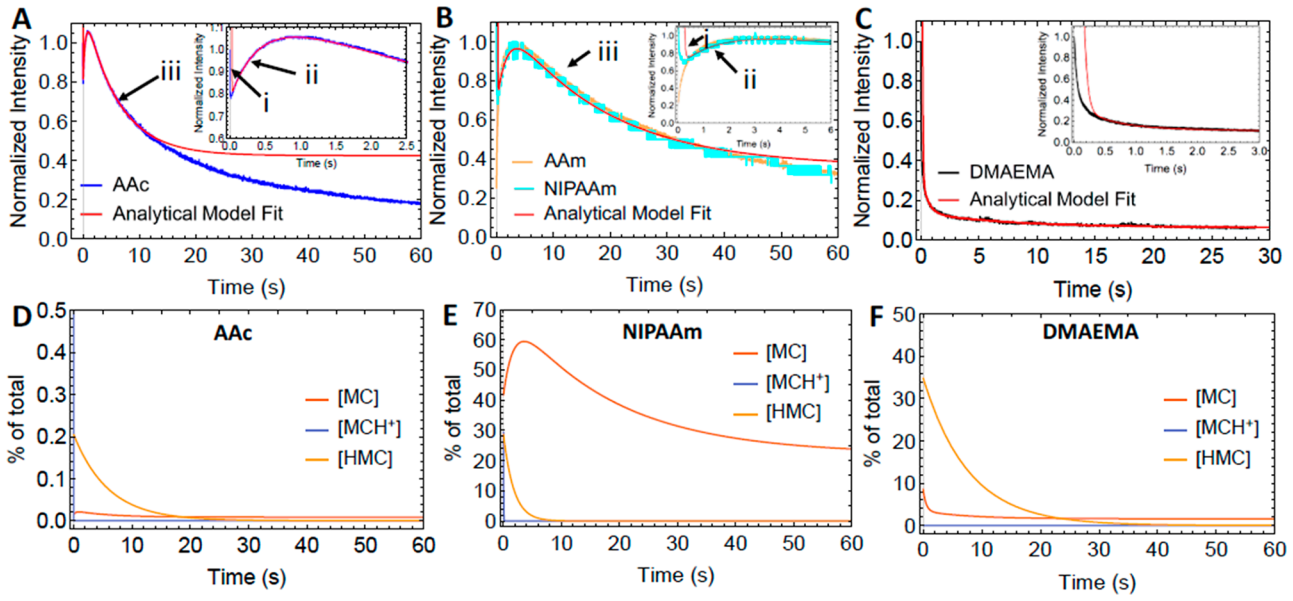

Figure 3. Example fits given by the analytical model incorporating aggregation/disaggregation to fluorescence dynamics data under high-intensity 405 nm excitation. (A) Analytical model fit to poly(AAc-*co*-SP) data. Fluorescence intensity is normalized to the initial fluorescence intensity. Inset shows a magnification of the first 2.5 s. (B) Analytical model fit to poly(NIPAAm-*co*-SP) data. Poly(AAm-*co*-SP) data are also shown. Fluorescence intensity of each data set is normalized to the maximum value after the first second of irradiation. Inset shows a magnification of the first 6 s. (C) Analytical model fit to poly(DMAEMA-*co*-SP) data. Fluorescence intensity is normalized to the initial fluorescence intensity. Inset shows a magnification of the first 3 s. (D) Model results of the MC, MCH^+, and H-MC concentration as a percentage of the total chromophore over time in the poly(AAc-*co*-SP) gel. While nearly 100% of initial chromophore is in the MCH^+ isomer, the graph *y*-axis is scaled to focus on the dynamics of the small amounts of MC and H-MC. (E) Model results of the MC, MCH^+, and H-MC concentration as a percentage of the total chromophore over time in the poly(NIPAAm-*co*-SP) gel. While the MCH^+ concentration drops nearly to zero very quickly, the modeled MC concentration increases by nearly 50% before decreasing over the course of several minutes. (F) Model results of the MC, MCH^+, and H-MC concentration as a percentage of the total chromophore over time in the poly(DMAEMA-*co*-SP) gel. The MCH^+ concentration is near zero due to the strongly basic internal gel environment. All model results use the parameters shown in Supporting Information Table S3.

the 470 nm peak allows for sufficient light-triggered disaggregation by 405 nm irradiation. By further assuming that the internal gel pH is constant, the dynamics of interconversion between the four species of our model can be reduced to a set of three coupled ordinary differential equations with parameters that depend on the total spiropyran concentration, the gel pH, the initial percentage of H-MC, the various reaction rates, and a scaling parameter used to match the arbitrary scale of the fluorescence data (for model details see Supporting Information section S7). These equations can be solved analytically to yield triexponential solutions. Estimates for the parameters were found by numerically fitting the analytical solutions to triexponential fits of the first 12−24 s of fluorescence intensity data for the spiropyran-functionalized pAAc, pNIPAAm, and pDMAEMA hydrogel high-intensity irradiation experiments. A separate fit was not found for the poly(AAm-*co*-SP) gel, as the initial increase in fluorescence upon irradiation is not compatible with the proposed model. However, the chemical similarities between AAm and NIPAAm and the observed similar slower fluorescence dynamics upon irradiation with high-intensity 405 nm light suggest that these materials likely share similar parameter values (for fitting details see Supporting Information section 7.2). Example fits are shown in Figure 3A−C. Some parameters, such as $k_{MCH\rightarrow SP}$ and $k_{HMC\rightarrow MC}$, were found to be directly related to one of the triexponential time scales and were thus highly constrained, while others, such as $k_{MC\rightarrow SP}$ and the pH, were found to have a range of possible values that led to excellent fits. For this reason, we focus on the general implications of the model rather than specific parameter values.

The reactions underlying each part of the observed dynamics can be identified by evaluating the dependence of each time scale on the parameters at the estimated fit values (Supporting Information section S7.4). A rapid decrease in fluorescence intensity initially occurs in all of the gels except for poly(AAm-*co*-SP) (Figure 3Ai,Bi), corresponding to the initial decrease in $[MCH^+]$ due to light-driven conversion of $MCH^+ \rightarrow$ SP. Fluorescence intensity then increases in poly(AAc-*co*-SP) (Figure 3Aii) with a time scale that depends on the rate of MC protonation, while in AAm- and NIPAAm-based gels it increases with a time scale determined by the rate of light-driven disaggregation, $k_{HMC\rightarrow MC}$ (Figure 3Bii). A subsequent slower loss of fluorescence intensity is observed, which in the poly(AAc-*co*-SP) gels occurs due to disaggregation of H-MC (Figure 3Aiii), while in poly(NIPAAm-*co*-SP) and poly(AAm-*co*-SP) (Figure 3Biii) we find that the slowest time scale is associated with the equilibration of MC and SP through a combination of direct isomerization of MC to SP and the indirect conversion of MC to SP through first being protonated and then photoconverted. The fitted rates broadly agree with the estimated rates determined using similar methods by Berton et al.,[28,39] although we note that the rate of protonation in all cases is estimated to be significantly slower than the rate suggested by ^{1}H NMR studies.

The model also explains the monotonically decreasing triexponential fluorescence intensity observed in poly(DMAEMA-*co*-SP) gels. In such gels we find that the rate of MC → SP isomerization is faster than disaggregation, so disaggregation does not lead to an increase in the concentration of MC. All of these dependencies are illustrated

https://doi.org/10.1021/jacs.1c08778
J. Am. Chem. Soc. 2022, 144, 219−227

by the response of each analytical fit to changes in parameter values, shown in Supporting Information section S7.4.

While we have shown that a model incorporating aggregates is able to explain the experimental observations, spiropyrans are also known to undergo pH-dependent hydrolysis in solution to form the respective Schiff's base and salicylaldehyde variant.[26,27,38,39] While the Schiff's base does not absorb at 405 nm or emit in the 525−575 nm spectral window, the absorption spectrum of the phenolate counterpart does tail into the 405 nm region, suggesting that any hydrolysis that occurs could create a measurable fluorescence signal in our experiments. However, we find that evidence for significant irreversible hydrolysis in our system is lacking and that irreversible hydrolysis is insufficient to explain the long term fluorescence dynamics after irradiation, especially the changes in fluorescence upon 561 nm excitation (see Supporting Information section S8 for a detailed discussion).

For example, in the spiropyran-containing pAAc, pAAm, and pNIPAAm gels, we observe a further and even slower decrease in the fluorescence at times greater than 30−60 s that deviates from the triexponential model. It is unlikely that this corresponds to an irreversible photodegradation process as we do not observe a persistent decrease in fluorescence compared to the background after long periods of intense irradiation and instead observe an increase in fluorescence (Supporting Information section S5). On the basis of this, we posit that these dynamics could be explained by aggregates existing in a spectrum of sizes and configurations, as has been suggested in the literature to explain similar observations,[31] but exploring this possibility is beyond the scope of this current work.

Importantly, our model can be used to estimate the concentrations of all species as a function of time during irradiation. The modeled concentrations of MC, MCH^+, and H-MC in poly(AAc-*co*-SP), poly(NIPAAm-*co*-SP), and poly(DMAEMA-*co*-SP) gels are shown in Figure 3D−F. In AAc- and NIPAAm-based gels, we see that the MCH^+ concentration drops down to essentially zero very quickly, reflecting the extremely fast light-driven conversion of MCH^+ to SP under high-intensity 405 nm irradiation. The concentration of H-MC also decreases monotonically, although at a slower rate. In contrast, the concentration of the MC isomer increases in both gels before slowly decreasing toward the photostationary state. In pAAc gels, this increase in MC concentration is insignificant due to the lower overall amount of chromophore found in the MC isomer, but in less acidic gels based on NIPAAm this effect is much more substantial. The MC isomer is highly hydrophilic, meaning an increase in the concentration of MC will counteract the gel contraction driven by the conversion of MCH^+ to SP. This could lead to an overall slower and lower magnitude response than in a more acidic gel with fewer aggregates and may be an important part of why spiropyran-functionalized pNIPAAm gels are found to have a larger and more repeatable response to irradiation when a small amount of acrylic acid is also included.[17] Our model extends beyond these observations to show how an acidic environment also affects the protonation rate and aggregate concentrations in ways that can potentially affect the overall response time and magnitude, especially under high-intensity monochromatic irradiation.

Understanding the Long Time Scale Fluorescence Behavior. The aggregation hypothesis can also explain the unexpected long-term fluorescence recovery dynamics observed after 405 nm excitation (see Figure 1C and Supporting Information section S5). Immediately after excitation, the gel undergoes a depletion of both MC and MCH^+ moieties relative to the background, leading to relatively lower fluorescence from both 405 and 561 nm excitation. However, a recovery of equilibrium between SP, MC, and MCH^+ concentrations occurs on the time scale of minutes, leaving the formation of H-MC to be the only unequilibrated process at longer time scales. It has been proposed that aggregation is a continuous process, starting with smaller aggregates that form more quickly and are only slightly blue-shifted relative to the MC peak.[31] These smaller aggregates may fluoresce under 561 nm light, which is closer to their less-shifted absorption peak, leading to the slowly increasing intensity of the irradiated spot in poly(AAc-*co*-SP) under 561 nm excitation. The irreversibility of this process after one month suggests that after disaggregation the system is not able to re-form the large initial aggregates. One possible explanation may be that these initial aggregates are formed prior to polymerization and so they may not be recoverable either due to the loss of unpolymerized spiropyran that was incorporated into the aggregate or due to thermodynamic barriers to the spontaneous formation of such aggregates by polymerized spiropyran. Instead, our observations suggest the slow formation of smaller aggregates involving fewer MC molecules. We note that while hydrolysis is also a slow and irreversible process,[26,27] the absorption of the hydrolysis products is far below the excitation wavelength of 561 nm and can thus be ruled out as a possible explanation for the long-term fluorescence behaviors.

CONCLUSIONS

The cooperative effects of co-monomer chemistry and spiropyran dynamics play a key role in the rational design of multiresponsive spiropyran-functionalized hydrogels under intense illumination. Under such conditions, the well-established MCH^+/MC/SP interconversion model falls short of explaining the nonmonotonic spiropyran dynamics. In order to elucidate these dynamics, we employed fluorescence microscopy to observe the switching of spiropyran moieties in a variety of responsive polymer hydrogel networks. The observed unusual nonmonotonic, triexponential fluorescence data cannot be explained by the MCH^+/MC/SP interconversion scheme considered previously in the literature. Instead, by invoking the existence of H-aggregated MC and incorporating their formation and disaggregation kinetics into a model of spiropyran isomerization, we were able to fit the observed fluorescence dynamics and to attribute each time scale to different transformations. We found that there is an initial fast conversion of MCH^+ to SP, followed by slower conversion of H-MC and MC to SP. This model provides insight into the ways that copolymerized moieties affect the spiropyran switching kinetics, a topic that has received relatively little attention in the literature[24,32] compared to direct modification of the spiropyran moiety.[1,10,18,26−28]

These results have important implications for the design and optimization of light-responsive hydrogels for small length scales, where the quadratic dependence of the time scale of poroelastic diffusion on the characteristic length scale can lead to a relatively fast response of the hydrogel. For example, at the micrometer scale of microfluidics,[1−5] mesoporous hydrogels,[43,48] or self-trapped beams,[14,15] the time scale of poroelastic diffusivity can be seconds or less. In these cases, the tens of seconds we observe to be required for complete

https://doi.org/10.1021/jacs.1c08778
J. Am. Chem. Soc. 2022, 144, 219−227

photoswitching even under high-intensity focused laser light becomes limiting to the full photoresponse. Furthermore, fast, complete reversibility is often highly desirable, in contrast to the slow rate of aggregation we observe.

The slow dynamics of disaggregation or MC protonation in nonacidic hydrogels can also be significant in applications where incident light must travel through a relatively thick spiropyran-functionalized hydrogel, even if the transverse length scale is small, such as in self-trapping of 20 μm wide beams through a 4 mm long gel.[14] In this case, photoconversion of MCH^+, MC, and H-MC decreases absorption of the incident beam, allowing it to propagate further into the material and cause further switching. Thus, considering the additional absorption caused by aggregates along with their slow disaggregation even under high-intensity irradiation will likely be necessary to fully understand the dynamics of these systems, unless aggregation is prevented.

On the basis of this, we conclude that pH and aggregation are important factors to consider when designing a multiresponsive spiropyran-functionalized hydrogel system. The importance of an acidic environment in achieving a large, reversible photoresponse has been demonstrated previously,[17] and by revealing the underlying interconversion network of spiropyran species, we elucidate precisely how an acidic environment creates a large equilibrium concentration of MCH^+ while aiding in the faster conversion of all merocyanine species into SP upon visible light irradiation.

Aggregation has not been previously suggested as an important factor in the photoactuation of spiropyran-functionalized hydrogels. While aggregation adds further complexity and responsivity to spiropyran-functionalized gel systems, which may be particularly interesting for the design of multistimuli-responsive and self-regulated smart actuators, it may be undesirable in simple actuators where long-term switching effects would interfere with actuator operation. In such cases, modified spiropyran moieties that do not aggregate should be used, such as doubly acrylated spiropyran cross-linkers[37] or spiropyrans with modified linkages that sterically impede aggregation.[41] These design considerations are broadly important for the use of multiresponsive spiropyran-functionalized hydrogels for applications in a wide variety of fields, including microfluidics,[1−5] soft robotics,[6] drug delivery,[13] and nonlinear optics.[14,15]

MATERIALS AND METHODS

Gel Synthesis. Acrylated spiropyran monomers were prepared as described in Supporting Information section S2. For all hydrogel samples 40 wt % of monomer was dissolved in 4:1 v/v DMSO/deionized water (DIW). To these solutions, 2% w/v *N*,*N*′-methylenebis(acrylamide) was added as a cross-linker. 0.49 wt % of acrylated spiropyran was dissolved in the prepolymer solution. Upon addition of 2-hydroxy-4′-(2-hydroxyethoxy)-2-methylpropiophenone as a photoinitiator, the hydrogel prepolymer solution was dispensed into a rectangular aluminum mold (approximately 10 mm × 4 mm × 1 mm), covered with a glass slide, and cured under a UV lamp at ambient temperature for 5 min. Cured hydrogel samples were then immersed in a large volume of deionized water to remove unreacted monomer and excess solvent. Irradiation and fluorescence experiments were conducted 1 day after gel synthesis.

Dissolved Polymer Preparation. Polymers for UV−vis experiments were prepared as described above except without *N*,*N*′-methylenebis(acrylamide) as a cross-linker and using a lower amount of photoinitiator. Prepolymer solutions of acrylamide and acrylic acid or 2-(dimethylamino)ethyl methacrylate were made with a 1:1 ratio of monomers by weight to volume. After polymerization 3 mL of DIW was added and polymers were being left in an orbital shaker at 50 °C for at least 8 h. See Supporting Information sections S3.2 and S3.3 for details.

Confocal Fluorescence. All measurements were taken on a Zeiss LSM 710 confocal microscope. Gel samples were immersed in deionized water in a polystyrene Petri dish, and a 10× Zeiss water immersion lens was used for imaging. For an excitation wavelength of λ_{ex} = 561 nm we measured fluorescence intensity in a window of 625−675 nm, while for λ_{ex} = 405 nm excitation we use a window of 525−575 nm. Excitation and fluorescence measurements can be done in a single focused spot or scanned over an area, and the excitation power can be controlled from μW to mW. For experiments we used two different intensities: a high intensity to observe light-driven switching dynamics, and a low intensity with short exposure times to observe dark thermally driven conversion dynamics. High-intensity experiments correspond to a power of 5.5 mW for 561 nm light and 4.7 mW for 405 nm light. Low-intensity experiments used a power of 9.1 μW for 561 nm light and 5.6 μW for 405 nm light. Laser power was measured with a PM120D Si photodiode power sensor (Thorlabs).

UV−Visible Spectroscopy. Buffer solutions for absorption measurements of the linear polymers were prepared at 0.2 M using appropriate amounts of citrate buffer for the pH range 3−6, and phosphate buffer for the pH range 6−8.5. These buffers were adjusted to their final pH with aqueous sodium hydroxide or hydrogen chloride solutions. Solutions of linear polymers were freshly prepared by diluting 35 μL of polymer solution in 2 mL of 0.2 M pH buffers. UV−vis spectra were obtained on an Agilent 8453 UV−vis diode array spectrophotometer equipped with a Peltier-based temperature-controlled cuvette holder (Agilent). Samples were measured in disposable PMMA or PS cuvettes of 10 mm path length. Spectra were baseline corrected for their absorption at 700 nm. UV−vis spectra of linear polymer solutions were normalized with respect to their absorption at 280 nm (Irgacure 2959). Data analysis was performed using GraphPad Prism, R (https://www.r-project.org/) and Spectragryph software.

Model Fitting. Single, biexponential, and triexponential models were fit to normalized fluorescence data using the built-in Wolfram Mathematica 11.3.0.0 FindFit function. In order to correct for the significantly different time scales observed in the triexponential fluorescence data, the data were split into three sections based on the location of the two local extrema and the same number of equally spaced samples were taken in each section. These resampled data were then used to find the triexponential fit.

Parameters for the species interconversion model including H-aggregates were estimated by fitting the analytical model parameters such that the triexponential prefactors and rate constants matched the triexponential fit. Fitting was done using the built-in Wolfram Mathematica 11.3.0.0 NMinimize function with the "RandomSearch" method to find a minimum of a normalized least-squares error function. A second round of minimization was conducted using random points chosen near the results of the initial minimization, and the median values of the resulting fit parameters were taken to estimate the most likely parameter values. See Supporting Information section S7.2 for more details.

ASSOCIATED CONTENT

Supporting Information

The Supporting Information is available free of charge at https://pubs.acs.org/doi/10.1021/jacs.1c08778.

Experimental procedures, characterization, and synthetic procedures for the spiropyran monoacrylate monomer, spiropyran-modified linear polymers, and hydrogels, laser scanning confocal fluorescence microscopy data, UV−vis absorption spectra, X-ray scattering data, and theoretical modeling (PDF)

https://doi.org/10.1021/jacs.1c08778
J. Am. Chem. Soc. 2022, 144, 219−227

AUTHOR INFORMATION

Corresponding Author

Joanna Aizenberg − *John A. Paulson School of Engineering and Applied Sciences, Harvard University, Cambridge, Massachusetts 02138, United States; Department of Chemistry and Chemical Biology, Harvard University, Cambridge, Massachusetts 02138, United States;* orcid.org/0000-0002-2343-8705; Email: jaiz@seas.harvard.edu

Authors

Amos Meeks − *John A. Paulson School of Engineering and Applied Sciences, Harvard University, Cambridge, Massachusetts 02138, United States;* orcid.org/0000-0002-8866-0489

Michael M. Lerch − *John A. Paulson School of Engineering and Applied Sciences, Harvard University, Cambridge, Massachusetts 02138, United States; Stratingh Institute for Chemistry, University of Groningen, 9747 AG Groningen, The Netherlands;* orcid.org/0000-0003-1765-0301

Thomas B. H. Schroeder − *John A. Paulson School of Engineering and Applied Sciences, Harvard University, Cambridge, Massachusetts 02138, United States*

Ankita Shastri − *Department of Chemistry and Chemical Biology, Harvard University, Cambridge, Massachusetts 02138, United States*

Complete contact information is available at: https://pubs.acs.org/10.1021/jacs.1c08778

Notes

The authors declare no competing financial interest.

ACKNOWLEDGMENTS

The work was supported by the U.S. Army Research Office (Award W911NF-17-1-0351). A.M. acknowledges a National Defense Science & Engineering Graduate (NDSEG) Fellowship from the U.S. Department of Defense (DoD). M.M.L. thanks the Netherlands Organisation for Scientific Research (NWO) for a Rubicon Fellowship (019.182EN.027), and T.B.H.S. acknowledges support from the Swiss National Science Foundation (Postdoc.Mobility Fellowship P400P2-180743). The authors are grateful to Michael Aizenberg and Mariangela Di Donato for fruitful discussions. The authors also thank Mikhail Zhernenkov and Guillaume Freychet for their help with X-ray scattering experiments. X-ray scattering measurements were performed at the Soft Matter Interfaces (12-ID, SMI) beamline of the National Synchrotron Light Source II (NSLS-II), a U.S. Department of Energy (DOE) Office of Science User Facility operated for the DOE Office of Science by Brookhaven National Laboratory (BNL) under Contract DE-SC0012704.

REFERENCES

(1) Ter Schiphorst, J.; et al. Molecular design of light-responsive hydrogels, for in situ generation of fast and reversible valves for microfluidic applications. *Chem. Mater.* **2015**, *27*, 5925−5931.

(2) Sugiura, S.; et al. On-demand microfluidic control by micropatterned light irradiation of a photoresponsive hydrogel sheet. *Lab Chip* **2009**, *9*, 196−198.

(3) Sumaru, K.; Takagi, T.; Sugiura, S.; Kanamori, T. Spiropyran-functionalized hydrogels. In *Soft Actuators*; Springer Singapore, 2019; pp 309−320, DOI: 10.1007/978-981-13-6850-9_17.

(4) Sugiura, S.; et al. Photoresponsive polymer gel microvalves controlled by local light irradiation. *Sens. Actuators, A* **2007**, *140*, 176−184.

(5) ter Schiphorst, J.; et al. Photoresponsive passive micromixers based on spiropyran size-tunable hydrogels. *Macromol. Rapid Commun.* **2018**, *39*, 1700086.

(6) Francis, W.; Dunne, A.; Delaney, C.; Florea, L.; Diamond, D. Spiropyran based hydrogels actuators—Walking in the light. *Sens. Actuators, B* **2017**, *250*, 608−616.

(7) Sutton, A.; et al. Photothermally triggered actuation of hybrid materials as a new platform for in vitro cell manipulation. *Nat. Commun.* **2017**, *8*, 14700.

(8) Stumpel, J. E.; Liu, D.; Broer, D. J.; Schenning, A. P. H. J. Photoswitchable hydrogel surface topographies by polymerisation-induced diffusion. *Chem. - Eur. J.* **2013**, *19*, 10922−10927.

(9) Stumpel, J. E.; et al. Photoswitchable ratchet surface topographies based on self-protonating spiropyran-NIPAAM hydrogels. *ACS Appl. Mater. Interfaces* **2014**, *6*, 7268−7274.

(10) Satoh, T.; Sumaru, K.; Takagi, T.; Kanamori, T. Fast-reversible light-driven hydrogels consisting of spirobenzopyran-functionalized poly(*N*-isopropylacrylamide). *Soft Matter* **2011**, *7*, 8030−8034.

(11) Joseph, G.; Pichardo, J.; Chen, G. Reversible photo-/thermoresponsive structured polymer surfaces modified with a spirobenzopyran-containing copolymer for tunable wettability. *Analyst* **2010**, *135*, 2303−2308.

(12) Wang, S.; Choi, M. S.; Kim, S. H. Bistable photoswitching in poly(*N*-isopropylacrylamide) with spironaphthoxazine hydrogel for optical data storage. *J. Photochem. Photobiol., A* **2008**, *198*, 150−155.

(13) Tong, R.; Hemmati, H. D.; Langer, R.; Kohane, D. S. Photoswitchable nanoparticles for triggered tissue penetration and drug delivery. *J. Am. Chem. Soc.* **2012**, *134*, 8848−8855.

(14) Morim, D. R.; et al. Opto-chemo-mechanical transduction in photoresponsive gels elicits switchable self-trapped beams with remote interactions. *Proc. Natl. Acad. Sci. U. S. A.* **2020**, *117*, 3953−3959.

(15) Meeks, A.; Mac, R.; Chathanat, S.; Aizenberg, J. Tunable long-range interactions between self-trapped beams driven by the thermal response of photoresponsive hydrogels. *Chem. Mater.* **2020**, *32*, 10594−10600.

(16) Klajn, R. Spiropyran-based dynamic materials. *Chem. Soc. Rev.* **2014**, *43*, 148−184.

(17) Ziółkowski, B.; Florea, L.; Theobald, J.; Benito-Lopez, F.; Diamond, D. Self-protonating spiropyran-*co*-NIPAM-*co*-acrylic acid hydrogel photoactuators. *Soft Matter* **2013**, *9*, 8754−8760.

(18) Li, C.; Iscen, A.; Palmer, L. C.; Schatz, G. C.; Stupp, S. I. Light-driven expansion of spiropyran hydrogels. *J. Am. Chem. Soc.* **2020**, *142*, 8447−8453.

(19) Volarić, J.; Szymanski, W.; Simeth, N. A.; Feringa, B. L. Molecular photoswitches in aqueous environments. *Chem. Soc. Rev.* **2021**, *50*, 12377-12449.

(20) Kortekaas, L.; Browne, W. R. The evolution of spiropyran: fundamentals and progress of an extraordinarily versatile photochrome. *Chem. Soc. Rev.* **2019**, *48*, 3406−3424.

(21) Ivanov, A. E.; Eremeev, N. L.; Wahlund, P. O.; Galaev, I. Y.; Mattiasson, B. Photosensitive copolymer of *N*-isopropylacrylamide and methacryloyl derivative of spyrobenzopyran. *Polymer* **2002**, *43*, 3819−3823.

(22) Garcia, A.; et al. Photo-, thermally, and pH-responsive microgels. *Langmuir* **2007**, *23*, 224−229.

(23) Wang, S.; Choi, M. S.; Kim, S. H. Multiple switching photochromic poly(*N*-isopropylacrylamide) with spironaphthoxazine hydrogel. *Dyes Pigm.* **2008**, *78*, 8−14.

(24) Achilleos, D. S.; Vamvakaki, M. Multiresponsive spiropyran-based copolymers synthesized by atom transfer radical polymerization. *Macromolecules* **2010**, *43*, 7073−7081.

(25) Shi, Z.; Peng, P.; Strohecker, D.; Liao, Y. Long-lived photoacid based upon a photochromic reaction. *J. Am. Chem. Soc.* **2011**, *133*, 14699−14703.

(26) Hammarson, M.; Nilsson, J. R.; Li, S.; Beke-Somfai, T.; Andréasson, J. Characterization of the thermal and photoinduced reactions of photochromic spiropyrans in aqueous solution. *J. Phys. Chem. B* **2013**, *117*, 13561−13571.
(27) Stafforst, T.; Hilvert, D. Kinetic characterization of spiropyrans in aqueous media. *Chem. Commun.* **2009**, *0*, 287−288.
(28) Berton, C.; et al. Thermodynamics and kinetics of protonated merocyanine photoacids in water. *Chem. Sci.* **2020**, *11*, 8457−8468.
(29) Kaiser, C.; Halbritter, T.; Heckel, A.; Wachtveitl, J. Thermal, photochromic and dynamic properties of water-soluble spiropyrans. *ChemistrySelect* **2017**, *2*, 4111−4123.
(30) Kaiser, C.; Halbritter, T.; Heckel, A.; Wachtveitl, J. Proton-transfer dynamics of photoacidic merocyanines in aqueous solution. *Chem. - Eur. J.* **2021**, *27*, 9160−9173.
(31) Such, G.; Evans, R. A.; Yee, L. H.; Davis, T. P. Factors influencing photochromism of spiro-compounds within polymeric matrices. *J. Macromol. Sci., Polym. Rev.* **2003**, *43*, 547−579.
(32) Feeney, M. J.; Thomas, S. W. Tuning the negative photochromism of water-soluble spiropyran polymers. *Macromolecules* **2018**, *51*, 8027−8037.
(33) Kim, P.; Zarzar, L. D.; He, X.; Grinthal, A.; Aizenberg, J. Hydrogel-Actuated Integrated Responsive Systems (HAIRS): Moving towards Adaptive Materials. *Curr. Opin. Solid State Mater. Sci.* **2011**, *15* (6), 236−245.
(34) He, X.; et al. Synthetic homeostatic materials with chemo-mechano-chemical self-regulation. *Nature* **2012**, *487*, 214−218.
(35) Kim, P.; Zarzar, L. D.; Khan, M.; Aizenberg, M.; Aizenberg, J. Environmentally responsive active optics based on hydrogel-actuated deformable mirror arrays. In *Proceedings of SPIE*; Schoenfeld, W. V., Wang, J. J., Loncar, M., Suleski, T. J., Eds.; SPIE, 2011; Vol. *7927*, 792705.
(36) Aizenberg, M.; Okeyoshi, K.; Aizenberg, J. Inverting the swelling trends in modular self-oscillating gels crosslinked by redox-active metal bipyridine complexes. *Adv. Funct. Mater.* **2018**, *28*, 1704205.
(37) Lerch, M.; Meeks, A.; Schroeder, T.; Shastri, A.; Aizenberg, J. From appendage to crosslinker − Unusual swelling behavior in spiropyran-modified hydrogels. *ChemRxiv* **2021**, DOI: 10.33774/chemrxiv-2021-s6k4c.
(38) Abeyrathna, N.; Liao, Y. Stability of merocyanine-type photoacids in aqueous solutions. *J. Phys. Org. Chem.* **2017**, *30*, e3664.
(39) Berton, C.; et al. Light-switchable buffers. *Angew. Chem., Int. Ed.* **2021**, *60*, 21737−21740.
(40) Goldburt, E.; Shvartsman, F.; Krongauz, V. 'Zipper' crystallization of polymers with spiropyran side groups. *Macromolecules* **1984**, *17*, 1876−1878.
(41) Goldburt, E.; Shvartsman, F.; Fishman, S.; Krongauz, V. Intramolecular interactions in photochromic spiropyran-merocyanine polymers. *Macromolecules* **1984**, *17*, 1225−1230.
(42) Sumaru, K.; Ohi, K.; Takagi, T.; Kanamori, T.; Shinbo, T. Photoresponsive properties of poly(*N*-isopropylacrylamide) hydrogel partly modified with spirobenzopyran. *Langmuir* **2006**, *22*, 4353−4356.
(43) Ziółkowski, B.; Florea, L.; Theobald, J.; Benito-Lopez, F.; Diamond, D. Porous self-protonating spiropyran-based NIPAAm gels with improved reswelling kinetics. *J. Mater. Sci.* **2016**, *51*, 1392−1399.
(44) Sato, H.; Shinohara, H.; Kobayashi, M.; Kiyokawa, T. Decomposition of merocyanine aggregates into monomers in UV-irradiated spiropyran solutions as revealed in anomalous absorption decay at the merocyanine monomer band. *Chem. Lett.* **1991**, *20*, 1205−1208.
(45) Würthner, F.; Kaiser, T. E.; Saha-Möller, C. R. J-aggregates: From serendipitous discovery to supramolecular engineering of functional dye materials. *Angew. Chem., Int. Ed.* **2011**, *50*, 3376−3410.
(46) Goldburt, E.; Krongauz, V. A simple relationship between rate of color change and molecular weight of a photochromic spiropyran polymer. *Macromolecules* **1986**, *19*, 246−247.
(47) Seki, T.; Ichimura, K. Formation of head-to-tail and side-by-side aggregates of photochromic spiropyrans in bilayer membrane. *J. Phys. Chem.* **1990**, *94*, 3769−3775.
(48) Eklund, A.; Zhang, H.; Zeng, H.; Priimagi, A.; Ikkala, O. Fast switching of bright whiteness in channeled hydrogel networks. *Adv. Funct. Mater.* **2020**, *30*, 2000754.